Dual Biochemical Oscillators May Control Cellular Reversals in *Myxococcus xanthus*

Erik Eckhert,[1,2] Padmini Rangamani,[3] Annie E. Davis,[2] George Oster,[2] and James E. Berleman[2,4, 5,*]

[1]University of California, Berkeley/University of California, San Francisco Joint Medical Program, Berkeley, California; [2]Department of Molecular and Cell Biology, University of California, Berkeley, Berkeley, California; [3]Department of Mechanical and Aerospace Engineering, University of California, San Diego, La Jolla, California; [4]Life Sciences Division, Lawrence Berkeley National Laboratory, Berkeley, California; [5]Department of Biology, St. Mary's College, Moraga, California.

Supplemental Materials

Table S1. Table of reactions and underlying assumptions For each term, equations with reaction details are presented. Our assumptions regarding the *associated cellular processes* are summarized as follows: (1) FrzF adds methyl groups to conserved Glu residues of FrzCD and FrzG removes them. (2) Activated FrzCD increases FrzE activity (autophosporylation of the conserved His residue). (3) Activated FrzE does phosphotransfer to conserved Asp residues on FrzZ and FrzG. (4) Active FrzZ has increased affinity for the Mgl pathway, decreasing the (GAP) activity of MglB, which facilitates the activation of MglA. (5) Because FrzCD, F, E, and Z mutants demonstrate *irregular* reversals, there is likely a secondary signal (mot) below the level of the Frz pathway acting on MglA. (6) Activated MglA activates the two motility systems through FrzS and AglZ. (7) FrzS positively regulates S-motors (not modeled) and also feeds back on MglA. AglZ positively regulates A-motors (not modeled) and also feeds back on both MglA and FrzCD. Our assumptions regarding model construction are summarized as follows: (1) All species are present in large enough quantities that the rates of reactions can be modeled using deterministic approaches. (2) Enzymatic reactions are modeled using Michaelis-Menten kinetics and other reactions are modeled using mass-action kinetics. (3) ATP concentration is present in large excess and is assumed to be constant during the time scale of the events modeled.

Note that the enzymes catalyzing a reaction are shown in **bold font**.

Reactions	**Kinetics**	**Underlying mechanisms and assumptions**	**References**
$FrzF \rightarrow FrzF^*$	First order reaction k_f= 1 s^{-1}	Conformational change of FrzF to FrzF*	[S1] (1)
$FrzF^* \rightarrow FrzF$	First order reaction k_f=4 s^{-1}	Conformational change of FrzF* to FrzF	[S1] (1)
$FrzG + \boldsymbol{FrzE}^* \rightarrow FrzG^*$	Enzymatic reactions K_M=5x10^{-3} μM k_{cat}=6 s^{-1}	His to Asp phosphorylation on FrzG catalyzed by FrzE*	(2) (2)
$FrzG^* \rightarrow FrzG$	First order reaction k_f=1 s^{-1}	Intrinsic phosphatase activity of FrzG* where the phosphotidyl-Asp bond is broken by water	(2) (2)

$FrzCD + \boldsymbol{FrzF}^* \rightarrow FrzCD^*$	Enzymatic reactions K_M=5x10^{-3} μM k_{cat}=1.3s^{-1}	Methylation reaction resulting in a conformational change of FrzCD, catalyzed by FrzF*	(52) (3)
$FrzCD^* + \boldsymbol{FrzG}^* \rightarrow FrzCD$	Enzymatic reactions K_M=5x10^{-3} μM k_{cat}=0.5 s^{-1}	Demethylation reaction resulting in a conformational change of FrzCD, catalyzed by FrzG*	(52) (3)
$FrzCD^* + \boldsymbol{AglZ}^* \rightarrow FrzCD$	Enzymatic reactions K_M=5x10^{-3} μM k_{cat}=0.5 s^{-1}	Conformational change assumed to be catalyzed by AglZ*	(38) (4)
$FrzE + \boldsymbol{FrzCD}^* \rightarrow FrzE^*$	Enzymatic reactions K_M=5x10^{-3} μM k_{cat}=6 s^{-1}	Protein-protein interaction between FrzE and FrzCD* leads to autophosphorylation by FrzE	(25) (5)
$FrzE^* + \boldsymbol{FrzZ}^* \rightarrow FrzE$	Enzymatic reactions K_M=5x10^{-3} μM k_{cat}=3 s^{-1}	His to Asp phosphorylation on FrzE* catalyzed by FrzZ*	(28) (6)
$FrzE^* + \boldsymbol{FrzG}^* \rightarrow FrzE$	Enzymatic reactions K_M=5x10^{-3} μM k_{cat}=3 s^{-1}	His to Asp phosphorylation on FrzE* catalyzed by FrzG*	(2) (2)
$FrzZ + \boldsymbol{FrzE}^* \rightarrow FrzZ^*$	Enzymatic reactions K_M=5x10^{-3} μM k_{cat}=5 s^{-1}	His to Asp phosphorylation on FrzZ catalyzed by FrzE*	(28) (6)
$FrzZ^* \rightarrow FrzZ$	First order reaction k_f=1 s^{-1}	Hydrolysis reaction	(6)
$MglB \rightarrow MglB^*$	First order reaction k_f=1.5 s^{-1}	Conformational change of MglB to MglB*	(7)

$MglB^* + \boldsymbol{FrzZ}^* \rightarrow MglB$	Enzymatic reactions K_M=5x10^{-3} μM k_{cat}=6 s^{-1}	Conformational change of MglB* to MglB mediated by FrzZ*	(3) (8)
$MglA + \boldsymbol{AglZ}^* \rightarrow MglA^*$	Enzymatic reactions K_M=5x10^{-3} μM k_{cat}=1 s^{-1}	Conformational change of MglA to MglA* assumed to be catalyzed byAglZ*	(32) (9)
$MglA + \boldsymbol{Mot} \rightarrow MglA^*$	Enzymatic reactions K_M=5x10^{-3} μM k_{cat}=1 s^{-1}	Conformational change of MglA to MglA* assumed to be catalyzed by MotA	(53) (10)
$MglA^* + \boldsymbol{MglB}^* \rightarrow MglA$	Enzymatic reactions K_M=5x10^{-3} μM k_{cat}=4 s^{-1}	GAP activity of MglB* results in MglA* being converted to MglA	(3) (8)
$MglA^* + \boldsymbol{FrzS}^* \rightarrow MglA$	Enzymatic reactions K_M=5x10^{-3} μM k_{cat}=4 s^{-1}	Conformational change of MglA* to MglA assumed to be catalyzed by FrzS*	(54) (11)
$AglZ + \boldsymbol{MglA}^* \rightarrow AglZ^*$	Enzymatic reactions K_M=5x10^{-3} μM k_{cat}=5 s^{-1}	Conformational change of AglZ to AglZ* catalyzed by MglA*	(32) (9)
$AglZ^* \rightarrow AglZ$	First order reaction k_f=1 s^{-1}	Conformational change of AglZ* to AglZ	[32] (9)
$FrzS + \boldsymbol{MglA}^* \rightarrow FrzS^*$	Enzymatic reactions K_M=5x10^{-3} μM k_{cat}=4 s^{-1}	Conformational change of FrzS to FrzS* catalyzed by MglA*	(33) (12)
$FrzS^* + \boldsymbol{FrzS} \rightarrow Frz\mathrm{S}$	Autocatalytic Enzymatic reactions K_M=5x10^{-3} μM k_{cat}=2 s^{-1}	Conformational change of FrzS* to FrzS by autocatalysis	(55) (13,14)

Figure S2.

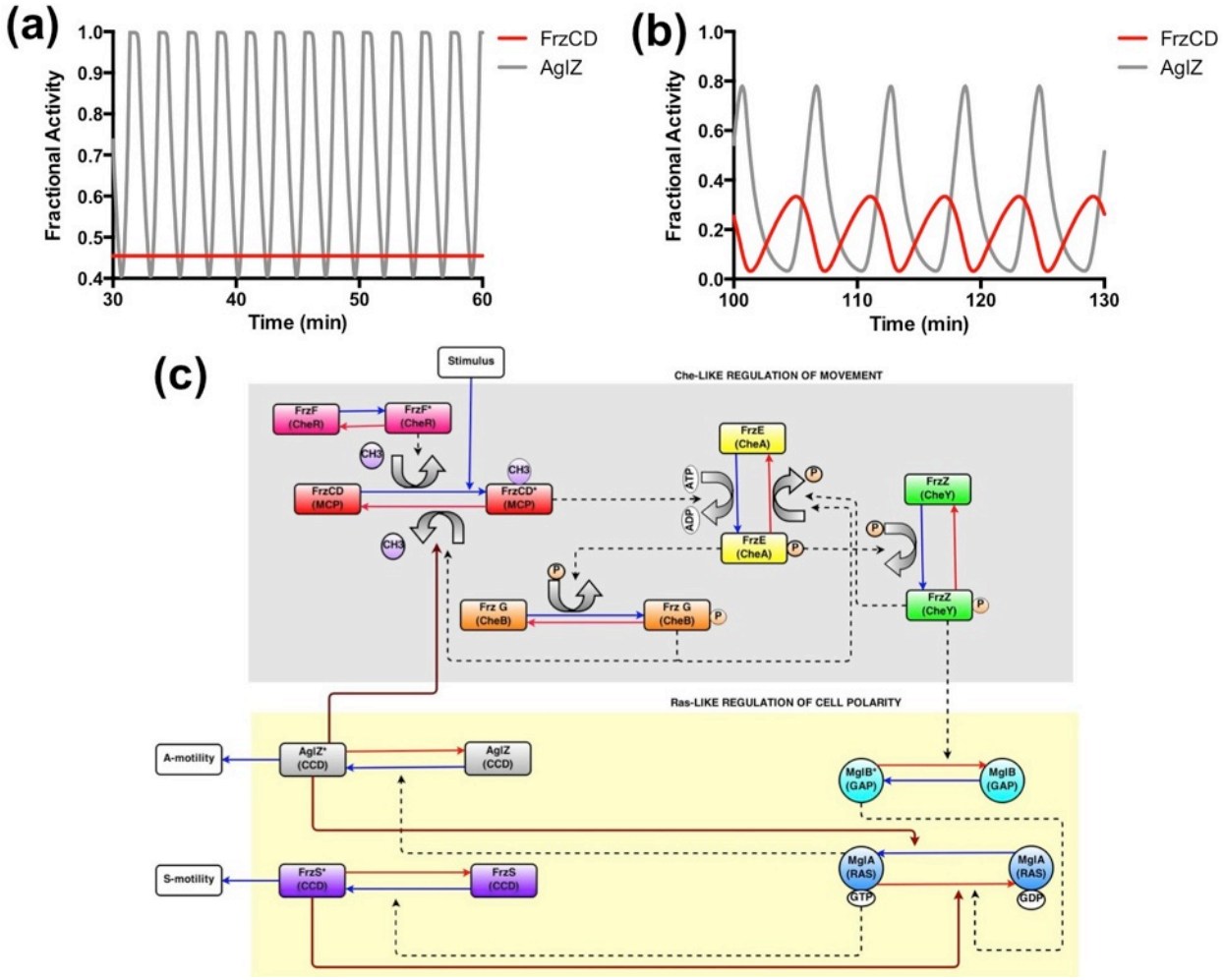

Figure S2. Model for disconnecting the two proposed feedback loops. When the two nested feedback loops that interact to produce wild type reversal periods of ~6 minutes are disconnected from each other, each is capable of producing oscillations of the motor pathway independently of the other. (a) Plot showing a decreased reversal period (~2.4 min) when AglZ-FrzCD feedback is terminated but the motor-MglA feedback is maintained. (b) Plot showing an increased reversal period (~6.1 min) when MglA-motor feedback is terminated but the AglZ-FrzCD feedback is maintained. (c) The reproduction of Figure 1b highlights (in burgundy) the feedback loops that were broken to produce the graphs shown here.

Figure S3.

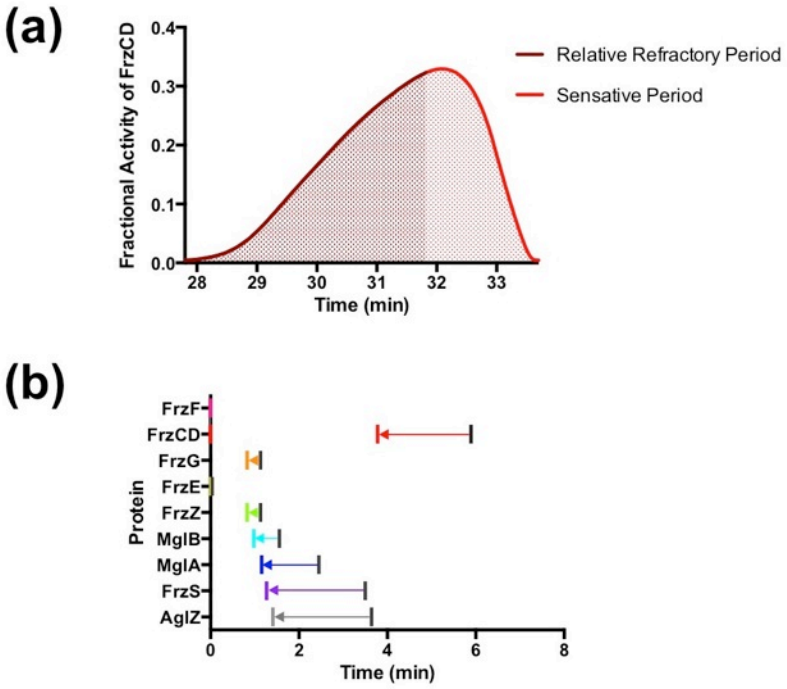

Figure S3. Refractory period and activation shift. In addition to oscillatory behavior in the basal state, the model should account for how behavior can change in response to a stimulus. (a) Graph of FrzCD over a single activity period with the sensitive and relative refractory periods labeled. Note that the cell can reverse faster in response to an external stimulus that occurs during the sensitive period compared to one in the relative refractory period. (b) The timing of protein activity, with respect to an oscillation cycle, shortens (see arrows) in response to an external stimulus during a relative refractory period. The grey lines denote protein activity without an external stimulus, as shown in Fig3a.

Table S4. Parameter values. A single parameter set can be used for all modeled behaviors (with the exception of the stimuli). Simulations over a wide range (up to several orders of magnitude) of initial conditions, Michaelis constants and maximum velocity constants lead us to believe the fundamental oscillatory behavior of the model is robust. The choice of parameters used in the model was based on comparison with available experimental data.

Figure	**Parameters**		
Fig. 3,4, SI1-2	Michaelis constants K=0.005	$FG_0 = CD_0 = E_0 = Z_0 = MglB_0 = MglA_0 = S_0 = AglZ_0 = 0.1$	
	$k_{F\,F}$=1	$k_{G\,F}^{max}$=6	$k_1 = 1.3$

	$k_{F\,R}$=4	$k_{G\,R}$=1	$k_{CD\,R}^{max}$=0.5
	$k_{E\,F}^{max}$=6	$k_{Z\,F}^{max}$=5	$k_{MglB\,F}$=1.5
	$k_{E\,R}^{max}$=3	$k_{Z\,R}$ = 1	$k_{MglB\,R}^{max}$=6
	$k_{MglA\,F}^{max}$=1	$k_{AglZ\,F}^{max}$=5	$k_{S\,F}^{max}$ = 4
	$k_{MglA\,R}^{max}$=4	$k_{Aglz\,R}$=1	$k_{S\,R}^{max}$=2
Fig. 6	k_2=0 (no external stimuli)	k_2=10 (external stimuli)	Δt=0.5 (a and b)
	Stim=3 (b)	Stim=4.238 (c)	Δt=10 (c)

Supporting References

1. Scott, A.E., E. Simon, S.K. Park, P. Andrews, and D.R. Zusman. 2008. Site-specific receptor methylation of FrzCD in Myxococcus xanthusis controlled by a tetra-trico peptide repeat (TPR) containing regulatory domain of the FrzF methyltransferase. Molecular Microbiology. 69: 724–735.

2. Bustamante, V.H., I. Martínez-Flores, H.C. Vlamakis, and D.R. Zusman. 2004. Analysis of the Frz signal transduction system of Myxococcus xanthus shows the importance of the conserved C-terminal region of the cytoplasmic chemoreceptor FrzCD in sensing signals. Molecular Microbiology. 53: 1501–1513.

3. McCleary, W.R., M.J. McBride, and D.R. Zusman. 1990. Developmental sensory transduction in Myxococcus xanthus involves methylation and demethylation of FrzCD. J. Bacteriol. 172: 4877–4887.

4. Mauriello, E.M.F., B. Nan, and D.R. Zusman. 2009. AglZ regulates adventurous (A-) motility in Myxococcus xanthus through its interaction with the cytoplasmic receptor, FrzCD. Molecular Microbiology. 72: 964–977.

5. Inclán, Y.F., S. Laurent, and D.R. Zusman. 2008. The receiver domain of FrzE, a CheA–CheY fusion protein, regulates the CheA histidine kinase activity and downstream signaling to the A- and S-motility systems of Myxococcus xanthus. Molecular Microbiology. 68: 1328–1339.

6. Inclán, Y.F., H.C. Vlamakis, and D.R. Zusman. 2007. FrzZ, a dual CheY-like response regulator, functions as an output for the Frz chemosensory pathway of Myxococcus xanthus. Molecular Microbiology. 65: 90–102.

7. Keilberg, D., K. Wuichet, F. Drescher, and L. Søgaard-Andersen. 2012. A Response Regulator Interfaces between the Frz Chemosensory System and the MglA/MglB GTPase/GAP Module to Regulate Polarity in Myxococcus xanthus. PLoS Genet. 8: e1002951.

8. Zhang, Y., M. Franco, A. Ducret, and T. Mignot. 2010. A Bacterial Ras-Like Small GTP-Binding Protein and Its Cognate GAP Establish a Dynamic Spatial Polarity

Axis to Control Directed Motility. PLoS Biol. 8: e1000430.

9. Yang, R., S. Bartle, R. Otto, A. Stassinopoulos, M. Rogers, et al. 2004. AglZ is a filament-forming coiled-coil protein required for adventurous gliding motility of Myxococcus xanthus. J. Bacteriol. 186: 6168–6178.

10. Fremgen, S.A., N.S. Burke, and P.L. Hartzell. 2010. Effects of site-directed mutagenesis of MglA on motility and swarming of Myxococcus xanthus. BMC Microbiology. 10: 295.

11. Mauriello, E.M.F., F. Mouhamar, B. Nan, A. Ducret, D. Dai, et al. 2009. Bacterial motility complexes require the actin-like protein, MreB and the Ras homologue, MglA. The EMBO Journal. 29: 1–12.

12. Thomasson, B., J. Link, A.G. Stassinopoulos, N. Burke, L. Plamann, et al. 2002. MglA, a small GTPase, interacts with a tyrosine kinase to control type IV pili-mediated motility and development of Myxococcus xanthus. Molecular Microbiology. 46: 1399–1413.

13. Mignot, T., J.P. Merlie, and D.R. Zusman. 2007. Two localization motifs mediate polar residence of FrzS during cell movement and reversals of Myxococcus xanthus. Molecular Microbiology. 65: 363–372.

14. Shi, R., L. McDonald, M. Cygler, and I. Ekiel. 2014. Coiled-Coil Helix Rotation Selects Repressing or Activating State of Transcriptional Regulator DhaR. Structure/Folding and Design. 22: 478–487.